

## Atomic Spalling of a van der Waals Nanomembrane

Ji-Yun Moon, Sang-Hoon Bae,\* and Jae-Hyun Lee\*



Cite This: *Acc. Chem. Res.* 2024, 57, 2826–2835



Read Online

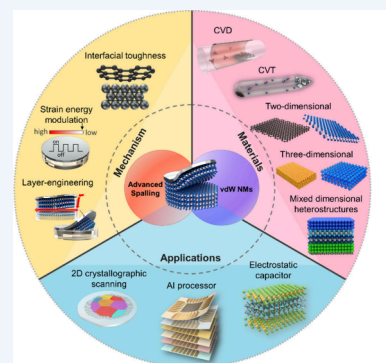
ACCESS |

Metrics & More

Article Recommendations

**CONSPECTUS:** The vertical integration of van der Waals nanomembranes (vdW NMs), composed of two-dimensional (2D) layered materials and three-dimensional (3D) freestanding films with vdW surfaces, opens new avenues for exploring novel physical phenomena and offers a promising pathway for prototyping ultrathin, superior-performance electronic and optoelectronic applications with unique functionalities. Achieving the desired functionality through vdW integration necessitates the production of high-quality individual vdW NMs, which is a fundamental prerequisite. A profound understanding of the synthetic strategies for vdW NMs, along with their fundamental working principles, is crucial in guiding the experimental design toward 3D integrated heterostructures. The foremost synthetic challenges in fabricating high-quality vdW NMs are achieving exact control over thickness and ensuring surface planarity on the atomic scale. Despite the development of numerous chemical and mechanical approaches to tackle these issues, an all-encompassing solution has yet to be realized. To address these challenges, we have developed advanced spalling techniques, specifically known as atomic spalling or 2D material-based layer transfer, which emerge as a promising technology for achieving both atomically precise thickness-engineered and atomically smooth vdW NMs. These techniques involve engineering the interfacial fracture toughness and strain energy in the vdW system, allowing for precise control over the initiation and the propagation of cracks within the vdW material based on controlled spalling theory.

In this Account, we summarize our recent advancements in the atomic precision spalling technique for the preparation of vdW NMs and their applications. We begin by introducing the fundamentals of advanced spalling techniques, which are based on spalling mode fracture in bilayer systems. Following this, we succinctly describe the preparation methods for source materials for vdW NMs, with a primary focus on chemical synthesis approaches. We then delve into the working principles underlying our recent contributions to advanced spalling techniques, providing insights into how this method attains unprecedented atomic-precision control compared to other fabrication methods with a particular emphasis on tuning the interface between the stressor and the vdW system. Subsequently, we highlight cutting-edge applications based on vdW heterostructures, which combine our spalled vdW NMs. Finally, we discuss the current challenges and future directions for advanced spalling techniques, underscoring their potential to be established as a robust methodology for the preparation of high-quality vdW NMs. Our advanced spalling strategy not only ensures the reliable production of vdW NMs with exceptional control over thickness and atomic-level flatness but also provides a robust theoretical framework essential for producing high-quality vdW NMs.



### KEY REFERENCES

- Shim, J.; Bae, S.-H.; Kong, W.; Lee, D.; Qiao, K.; Nezich, D.; Park, Y. J.; Zhao, R.; Sundaram, S.; Li, X.; Yeon, H.; Choi, C.; Kum, H.; Yue, R.; Zhou, G.; Ou, Y.; Lee, K.; Moodera, J.; Zhao, X.; Ahn, J.-H.; Hinkle, C.; Ougazzaden, A.; Kim, J. Controlled crack propagation for atomic precision handling of wafer-scale two-dimensional materials. *Science* **2018**, 362(6415), 665–670.<sup>1</sup> First demonstration of a layer-resolved splitting of wafer-scale monolayer 2D vdW NMs from an as-synthesized multilayer vdW film by incorporating the spalling theory.
- Moon, J.-Y.; Kim, M.; Kim, S.-I.; Xu, S.; Choi, J.-H.; Whang, D.; Watanabe, K.; Taniguchi, T.; Park, D. S.; Seo, J.; Cho, S. H.; Son, S.-K.; Lee, J.-H. Layer-engineered large-area exfoliation of graphene. *Sci. Adv.* **2020**, 6(44), eabc6601.<sup>2</sup> First demonstration to control the crack propagation depth in the vdW system by adjusting the interfacial toughness of the stressor film with a defect-free vdW surface.
- Moon, J.-Y.; Kim, D.-H.; Kim, S.-I.; Hwang, H.-S.; Choi, J.-H.; Hyeong, S.-K.; Ghods, S.; Park, H. G.; Kim, E.-T.; Bae, S.; Lee, S.-K.; Son, S.-K.; Lee, J.-H. Layer-engineered atomic-scale spalling of 2D van der Waals crystals. *Matter* **2022**, 5(11), 3935–3946.<sup>3</sup> Theoretically

Received: July 3, 2024

Revised: August 30, 2024

Accepted: September 3, 2024

Published: September 12, 2024



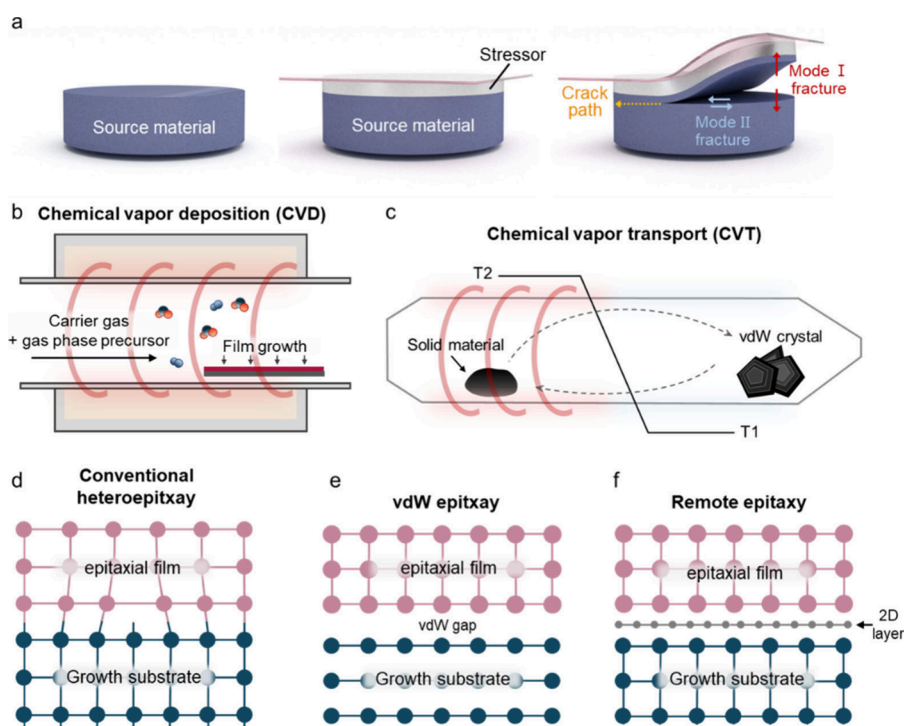


**Figure 1.** Spalling mode fracture in bilayer system and preparation of source materials for 2D, 3D vdW NMs. (a) Schematic illustration of the controlled spalling process in a bilayer film. (b, c) Schematic illustration of source material preparation methods for 2D vdW NMs: chemical vapor deposition (CVD) and chemical vapor transport (CVT), respectively. (d–f) Schematic of three different types of source material preparation methods for 3D vdW NMs: conventional heteroepitaxy, vdW epitaxy and remote epitaxy.

and experimentally elucidating the crack propagation behavior in the vdW system. Crack propagation in vdW materials can be controlled at the atomic level by fine-tuning the key elements such as the internal stress of the stressor film.

- Moon, J.-Y.; Kim, S.-I.; Ghods, S.; Park, S.; Kim, S.; Chang, S.; Jang, H. C.; Choi, J.-H.; Kim, J. S.; Bae, S.-H.; Whang, D.; Kim, T.-H.; Lee, J.-H. Nondestructive Single-Atom-Thick Crystallographic Scanner via Sticky-Note-Like van der Waals Assembling–Disassembling. *Adv. Mater.* **2024**, *36*, 2400091. <sup>4</sup> Representative application of advanced spalling for nondestructive crystallographic scanning of polycrystalline graphene.

## 1. INTRODUCTION

van der Waals nanomembranes (vdW NMs) refer to material platforms with thicknesses ranging from the atomic scale to a few hundred nanometers, possessing naturally or artificially terminated vdW interfaces.<sup>5,6</sup> Originally, the concept of vdW NMs was predominantly associated with two-dimensional layered materials (2D vdW NMs), but the recent advent of freestanding three-dimensional single-crystalline films (3D vdW NMs), which uniquely combine robust internal chemical bonds with clearly terminated physical bonds at their boundaries, has expanded the boundaries of this concept.<sup>6–8</sup> The most notable feature of these vdW NMs lies in their clean vdW interface and outstanding mechanical properties, including high stiffness and Young's modulus, originating from their thinness.<sup>9</sup> These distinctive characteristics enable ease material integration approaches through the simple vertical assembly of disparate materials without any restriction of lattice matching or the requirement for optimal synthetic

conditions, thereby introducing the innovative idea of vdW heterostructures.<sup>8,10,11</sup>

To date, various combinations of vdW NMs have been integrated into vdW heterostructures with diverse functionalities, facilitating the exploration of unprecedented physical phenomena and the successful prototyping of multifunctional devices.<sup>12,13</sup> These advancements have truly revolutionized multidisciplinary fields over material science, condensed matter physics, and electrical engineering and present ongoing opportunities for scientific and technological innovation. To seize these opportunities and fully exploit the potential of vdW heterostructures, the preparation of high-quality individual NMs should be a fundamental and essential prerequisite.

To achieve high-quality vdW NMs, recent synthetic challenges lie in the accurate control of their thickness and surface planarity. For 2D vdW NMs, the electronic structure undergoes dramatic changes depending on their thickness.<sup>14,15</sup> While 3D vdW NMs largely maintain consistent properties irrespective of thickness, their surface irregularities, when compared to the ultraflat surfaces of 2D vdW NMs, can result in incomplete interfacing, thus deteriorating the stability of the vdW heterostructure and impeding efficient charge transport. Several approaches have been proposed to produce vdW NMs and grapple with these challenges, such as chemical synthesis and mechanical exfoliation for 2D vdW NMs and techniques such as chemical, optical, and mechanical lift-off for 3D vdW NMs.<sup>16–20</sup> However, they have encountered fundamental limitations, including inaccurate control of thickness and limited material selection.

Recently, a novel synthetic approach known as advanced spalling has emerged as a promising solution to meet the stringent requirements for high-quality 2D and 3D vdW NMs.<sup>2,3,21</sup> Conventionally, spalling is an approach to separate

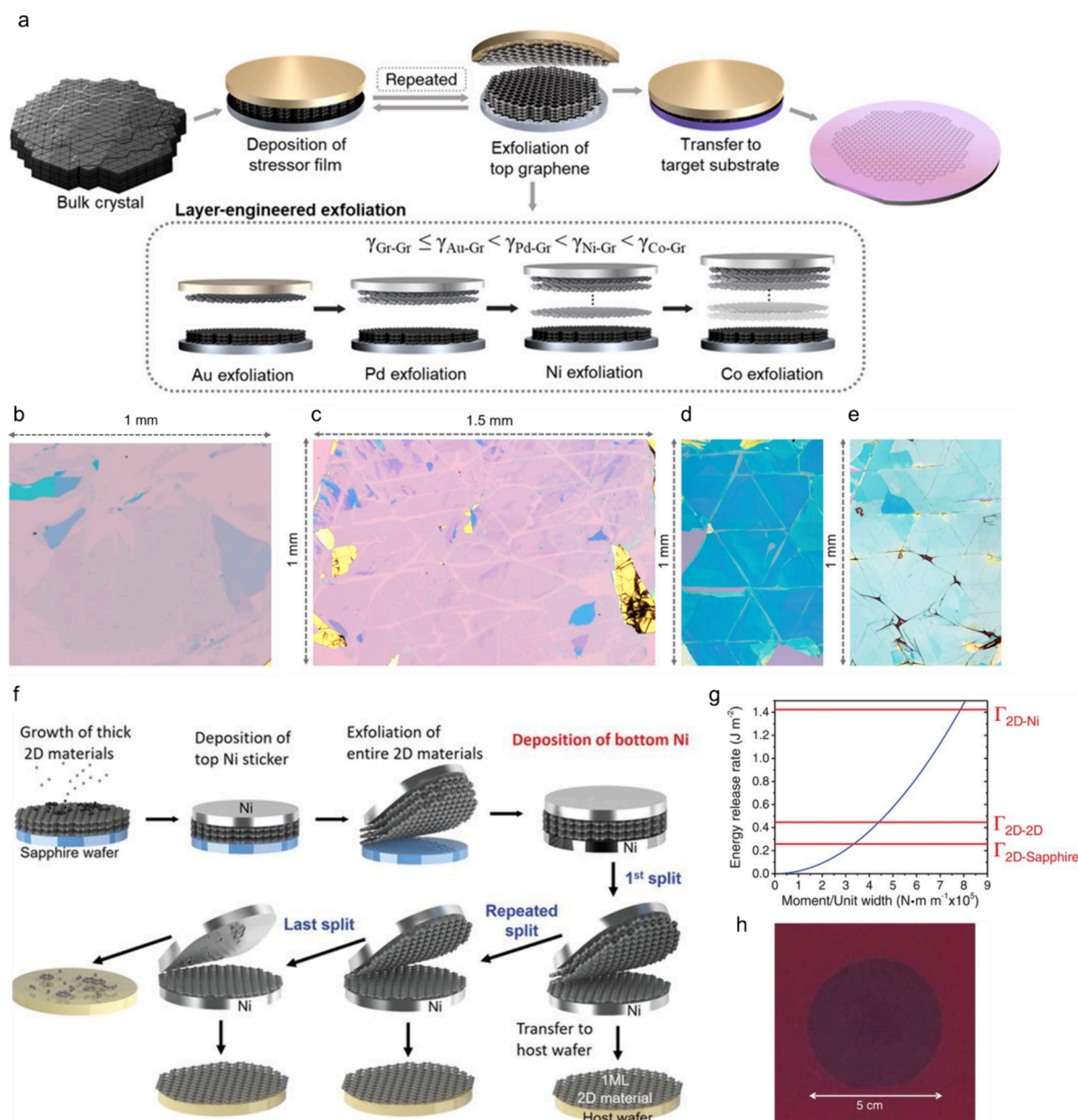


**Figure 2.** Atomic precision spalling of vdW NMs through adjusting binding energy. (a) Schematic illustration of layer-engineered spalling of graphene by using a metal stressor with different binding energies ( $\gamma$ ). The inset illustrates the change in the number of exfoliated graphene layers depending on the relative binding energy between the metal stressor film and graphite. (b–e) Optical images of spalled graphene from graphite using Au, Pd, Ni, and Co stressors, respectively. (f) Schematic illustration of selectively harvesting a monolayer 2D vdW NM from multilayer 2D vdW NM grown on a sapphire substrate by stepwise binding energy engineering. (g) Binding energy difference in 2D-Ni, 2D-2D, and 2D-sapphire interfaces. (h) Photograph of transferred  $\text{WS}_2$  monolayer with a lateral dimension of 5 cm on an oxidized silicon wafer. (Reproduced from refs 1 and 2. Copyrights 2018 and 2020 AAAS.)

thin layers from their source materials by mechanically fracturing them off with the help of a stressor film to control the crack propagation depth.<sup>22,23</sup> Advanced spalling refines these spalling techniques by integrating the adjustment of binding energy and internal stress parameters of the system, allowing for atomic-level flatness and precise thickness control of vdW NMs.

In the following sections, we aim to comprehensively cover the basics of advanced spalling techniques in our recent contributions to produce ideal vdW NMs. First, we introduce the fundamentals of advanced spalling, focusing on its working mechanism and preparation of source materials. We then explain the essential elements for designing the advanced

spalling technique, emphasizing binding energy and internal stress engineering. Subsequently, we present our representative research examples of atomically precise spalled vdW NMs for applications across various fields. Finally, we discuss future prospects of the technology, highlighting potential advancements and challenges that lie ahead.

## 2. FUNDAMENTALS OF ADVANCED SPALLING

### 2.1. Working Principles of Advanced Spalling

The working principle of advanced spalling techniques fundamentally follows the fracture mode of conventional controlled spalling in a bilayer system (Figure 1a).<sup>20,24,25</sup> To

achieve successful controlled spalling, the following key components are required: (i) a stressor, which is a thin metal film deposited on the surface of source materials with sufficient adhesion, (ii) brittle source materials, where the surfaces of the source materials will be separated by a stressor to produce the vdW NMs, and (iii) the application of external force, which is necessary for generating reliable crack initiation in the source material. A flexible handle layer (e.g., tape) is applied to the surface of the stressor/source material stack. By gently applying a slight force to the handle layer, a crack is initiated in the substrate at the edge of the stressor layer. The crack tip formed by crack initiation will guide the crack propagation, as the handle layer is mechanically guided, resulting in the separation of the desired thickness of the vdW NM from the source material.

When an external force is applied to the stressor/source material stack, a crack is initiated within the source material and propagates downward due to the mixed mode fracture of modes I (opening mode) and II (shearing mode). Under thermodynamic equilibrium conditions, where the shearing mode is minimized, the crack tip no longer propagates downward but instead grows parallel to the interface between the stressor and the source material. Once the crack tip reaches the edge of the source material from the initial crack point, the top surface of the source material is completely separated. The crack depth, which determines the thickness of the vdW NM, is dictated by the physical parameters of the source material and the stressor.

## 2.2. Preparation of Source Materials

As mentioned above, in the advanced spalling technique, vdW NMs are obtained by selectively exfoliating the top surface of the source material by using a stressor. Generally, thick vdW NM grown on substrate or bulk vdW crystals are used as source materials, and their preparation methods primarily rely on chemical synthetic approaches.

In the case of preparing source material for 2D vdW NMs, several growth methods, including chemical vapor deposition (CVD) and chemical vapor transport (CVT), have been widely adopted (Figure 1b,c). The CVD technique provides a versatile and scalable route to preparing thick 2D films (with multilayer thickness) on substrates.<sup>26,27</sup> This is achieved through the chemical reaction of gas-phase precursors, where growth parameters such as the vapor pressure, processing temperature, and precursor concentration are manipulated. These variables influence the nucleation and growth rates, surface diffusion of adatoms, and incorporation of precursor molecules into the growing film, ultimately affecting the crystallinity and defect density of the resulting 2D vdW NMs. Meanwhile, to utilize single-crystal bulk vdW crystals as source materials, the CVT technique is well-suited.<sup>28</sup> CVT growth is a mature technique for crystallizing nonvolatile solids, involving a chemical reaction that converts a condensed phase to a gaseous phase at elevated temperatures followed by recondensation into a crystalline solid at lower temperatures. This allows the precise control of crystal growth, synthesizing a variety of high-purity vdW crystals that do not naturally exist. Additionally, other synthetic methods such as flux-grown methods and molecular beam epitaxy (MBE) can be employed to prepare source materials for 2D vdW NMs.<sup>29,30</sup>

For the source material for 3D vdW NMs, various epitaxy techniques to realize clearly terminated physical bonds at the surface can be employed. Typically, the preparation of source

materials for 3D vdW NMs has relied on conventional heteroepitaxy, which requires strict conditions, such as low lattice mismatch, similar thermal expansion coefficients, and the same crystal structure between the epilayer and the growth substrate, thereby limiting the realization of varied source materials (Figure 1d). However, the recent development of advanced epitaxy techniques, such as vdW epitaxy and remote epitaxy, has expanded the range of possible source materials (Figure 1e,f).<sup>21,31</sup> These techniques leverage the vdW interface to alleviate the exacting growth requirement while improving the quality of source materials, resulting in fewer lattice mismatch-related defects such as threading dislocations in the epilayer.<sup>32,33</sup>

## 3. DESIGN OF ATOMIC-PRECISION ADVANCED SPALLING FROM SOURCE MATERIALS

### 3.1. Adjusting Binding Energy at the Interface

One of the most critical parameters for designing atomic precise spalling is the binding energy at the interface between stressor and source materials. In our group, we successfully separated graphene layers from graphite with atomic precision of thickness by adjusting the binding energy ( $\gamma$ ) between graphene and the stressor (Figure 2a).<sup>2,34</sup> By using different metal stressors, each with a different magnitude of binding energy with graphene, we simply controlled the spalling depth, resulting in precise control of the number of graphene layers.<sup>35,36</sup> When a Au stressor, which has a binding energy ( $\gamma_{\text{Au-Gr}} = 30$  meV/atom) similar to the interlayer vdW energy of graphite ( $\gamma_{\text{Gr-Gr}} = 21\text{--}25$  meV/atom), was deposited on freshly cleaved graphite, the topmost graphene monolayer was selectively exfoliated (Figure 2b). In contrast, by the deposition of different metal films (Pd, Ni, and Co) that have higher binding energy ( $\gamma_{\text{Pd-Gr}} = 84$  meV/atom,  $\gamma_{\text{Ni-Gr}} = 125$  meV/atom, and  $\gamma_{\text{Co-Gr}} = 160$  meV/atom) than the Au film, graphene with a controlled number of layers was obtained; the higher the binding energy, the deeper the spalling depth (Figure 2c–e). The graphene samples exfoliated with Pd, Ni, and Co stressors measured in thickness as bilayer, 7 nm, and 13 nm, respectively. Additionally, the Raman spectra of all spalled graphene samples showed an absence of the disorder-related D peak near  $1350\text{ cm}^{-1}$ , indicating their excellent crystallinity.

This approach of adjusting the binding energy to harvest desired thicknesses of 2D vdW NMs can be applied not only to vdW crystals but also to multilayer 2D vdW NMs grown on rigid substrates.<sup>1</sup> For example, layer-resolved splitting through stepwise control of binding energy provides a universal method for producing monolayer 2D vdW NMs at the wafer scale including MoS<sub>2</sub>, MoSe<sub>2</sub>, WS<sub>2</sub>, WSe<sub>2</sub>, and h-BN (Figure 2f). In this process, first a Ni stressor is deposited on top of the multilayer 2D vdW NMs/sapphire substrate. Since the binding energy of the Ni/2D interface is  $1.4\text{ J/m}^2$ , which is much higher than that of the 2D/sapphire ( $0.26\text{ J/m}^2$ ) and 2D/2D interfaces ( $0.45\text{ J/m}^2$ ), crack initiation occurs at the most vulnerable 2D/sapphire interface (Figure 2g). Then the crack propagates downward and along the 2D/sapphire interface, result in exfoliating the entire multilayer 2D vdW NM from the sapphire substrate. Subsequently, another Ni stressor is redeposited on the bottom of the exfoliated 2D multilayer, causing an additional spalling mode fracture. As the binding energy of the 2D/Ni interface is substantially higher than that of the 2D/2D interface, the cracks propagate through the

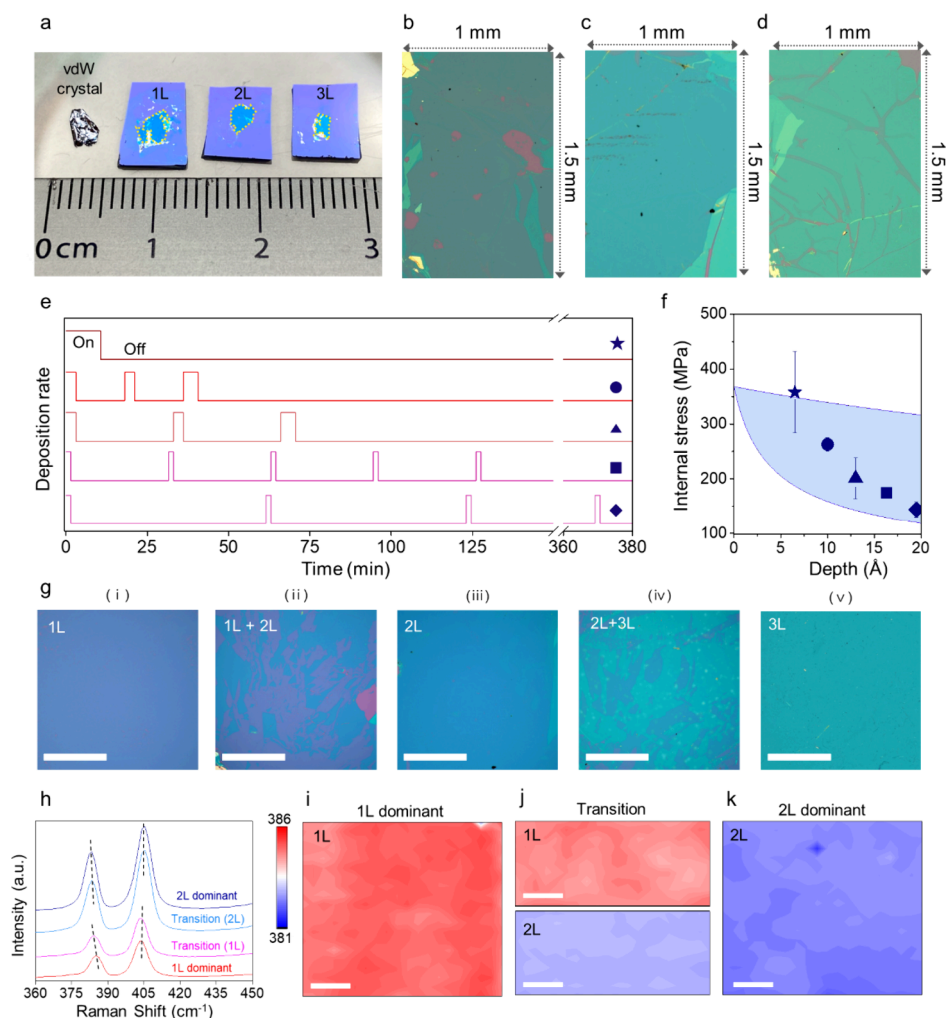


**Figure 3.** Atomic precision spalling of 2D vdW NMs through the internal stress modulation of a stressor film. (a) Photograph of spalled mono-, bi-, and trilayer MoS<sub>2</sub> from their bulk vdW crystal. (b–d) Optical images of spalled mono-, bi-, and trilayer MoS<sub>2</sub>. (e) Five different stress release times for modulating the internal stress of the Ag stressor film. (f) Plot of spalled depth versus internal stress of the Ag stressor film. (g) Optical images of the spalled MoS<sub>2</sub> with different stress release times introduced during the stressor deposition process. Scale bars are 100 μm. (h–k) Raman spectrum and Raman map of spalled mono- and bilayer MoS<sub>2</sub> with the transition region. (Reproduced from ref 3. Copyrights 2022 Elsevier.)

weaker 2D/2D interface directly above the bottom Ni layer, resulting in only a monolayer 2D being left on the bottom Ni stressor. By repeatedly adjusting the binding energy during each spalling mode fracture process, atomically precise layer-by-layer exfoliation of monolayer 2D vdW NMs from the multilayer can be achieved. Figure 2h shows a harvested monolayer WSe<sub>2</sub> on a SiO<sub>2</sub> substrate, which has a uniform and smooth surface with a root-mean-square (RMS) value of 0.5 nm.

Similarly, it was reported that an epitaxially grown 1.2 monolayer graphene film on SiC, composed of a graphene monolayer sheet and around 20% bilayer strips, can be separated into pure monolayer graphene through the sequential application of stressors with different interfacial binding energies. By use of a Ni stressor, the entire 1.2-layer graphene film was released from the SiC substrate. Subsequently, applying an Au stressor completely removed the bilayer strips from the graphene sheet, leaving only the monolayer graphene.<sup>37</sup>

The same principle of binding energy engineering can be extended to create high-quality 3D vdW materials with an exceptional surface flatness. Recently, the development of

remote epitaxy, where epitaxy takes place on a substrate coated with an atomic 2D layer, which is typically continuous monolayer graphene, has not only enabled the growth of heteroepitaxial films with less concern regarding lattice mismatch but also allows for the facile separation of the epitaxial layer.<sup>7,38,39</sup> While the interior of the epilayer is bonded by strong chemical bonds, there is vdW bonding at the interface between the epilayer and the 2D layer. The extremely low binding energy at this vdW interface acts as a crack initiation and propagation path during spalling mode fracture. As a result, the epilayer is quickly and accurately released along the vdW interface, generating freestanding 3D vdW NMs with atomically flat surfaces.

However, despite these advantages, remote epitaxy can be applied only to polarized materials such as compound semiconductors and complex oxide. More recently, graphene nanopatterns have been introduced as an advanced platform for the epitaxy technique, enabling the creation of a broad range of freestanding single-crystalline 3D vdW NMs including nonpolar elemental materials such as Ge.<sup>40</sup> Graphene nanopatterns allow the lateral overgrowth of elemental semi-

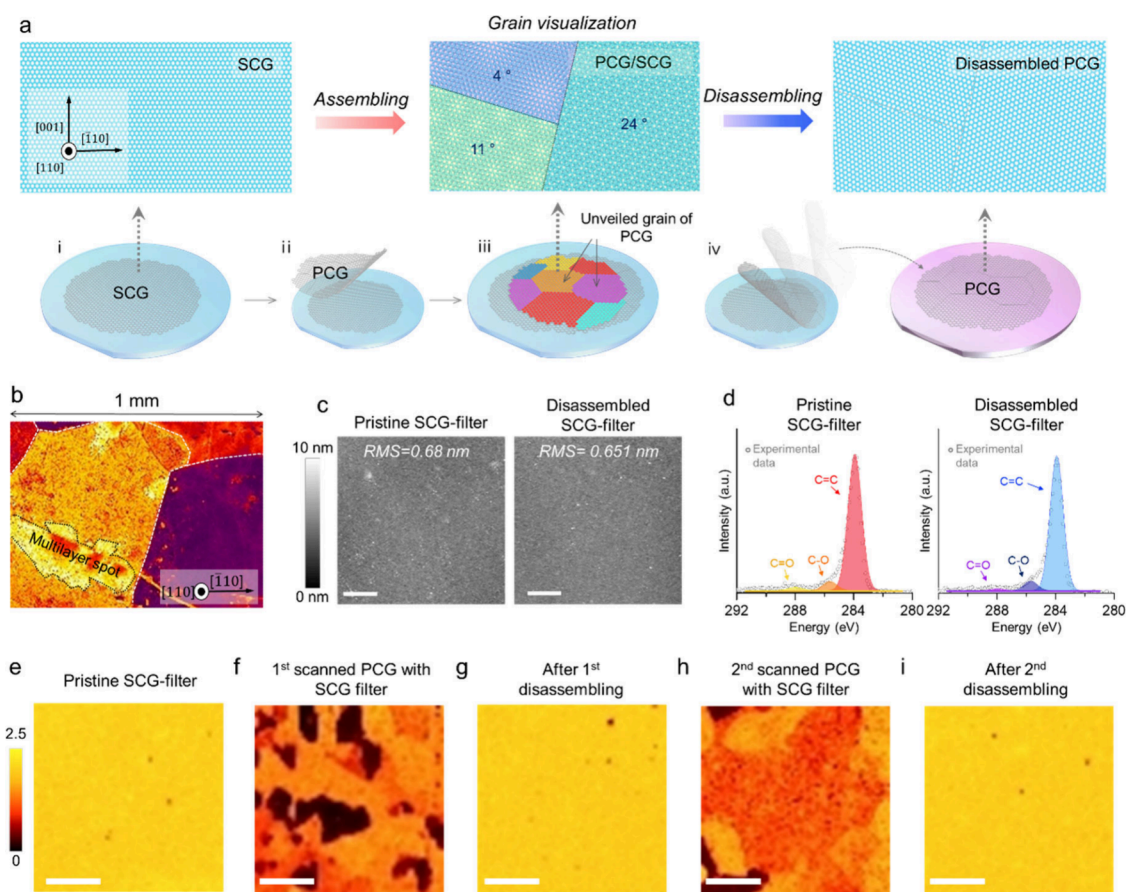


**Figure 4.** Nondestructive 2D crystallographic scanning. (a) Schematic illustration of the 2D crystallographic scanning process. (b) Raman mapping image of  $I(2D)/I(G)$  for an assembled PCG/SCG sample. (c, d) Representative AFM images and XPS spectra of pristine SCG (before assembling) and SCG after disassembling. The scale bars in the AFM images are  $5 \mu\text{m}$ . The AFM and XPS results show no significant changes before and after the vdW assembly and disassembly processes. (e–i) Multiple vdW assemblies and disassemblies conducted on the same SCG sample. (Reproduced from ref 4. Copyrights 2024 Wiley).

conductors on wafers while maintaining a reduced binding energy between the epitaxial layer and the graphene.

### 3.2. Modulating the Internal Stress of Stressors

Another key parameter for designing atomically precise spalling is the internal stress of stressors. In our previous reports, we precisely controlled the crack propagation path within vdW crystals through internal stress engineering, allowing us to selectively exfoliate mono- to trilayer  $\text{MoS}_2$  from their vdW crystals (Figure 3a–d).<sup>3,41</sup> A 70-nm-thick Ag thin film was chosen as the stressor material due to several advantages: (i) Since Ag is a noble metal, there is no need to consider the side effects of oxidation at the interface with the 2D material. (ii) The magnitude of the binding energy between Ag and the 2D vdW NMs is similar to the vdW energy. (iii) The internal stress of the Ag film can be readily tailored by tuning the deposition parameter during the deposition process.

In the process of Ag film growth using the Volmer–Weber mode, it is well established that the evolution of the internal stress changes dynamically. In the early stage of growth (less than 4 to 5 nm), before the film has coalesced, the film stress is compressive because of the surface capillary forces on the isolated clusters. At the point of island coalescence, tensile stress develops, associated with the formation of grain boundaries. When the film becomes continuous, the tensile stress decreases and shifts in a compressive direction until the

end of the deposition. If the growth is interrupted at this point, then internal stress relaxation occurs, and the film stress jumps to a less compressive value.<sup>42</sup> Therefore, by introducing a temporary interruption in the deposition process and controlling the duration of this period, we can modulate both the magnitude and direction of the internal stress in the Ag film. We refer to this temporary interruption as the “stress release time”. Ag stressors with stress release time showed lower internal stress compared to the continuously deposited Ag stressor, with internal stress decreasing gradually as the stress release time increased. As a result, the internal stress of Ag stressors at the same thickness can be modulated from about 430 to 150 MPa (Figure 3e,f).

Since the spalling depth is determined by balancing the total accumulated strain energy in the Ag stressor/top  $\text{MoS}_2$  layer with the binding energy of the  $\text{MoS}_2$  crystal, which represents the thermodynamic equilibrium condition, we were able to control the number of spalled  $\text{MoS}_2$  layers by adjusting the internal stress.<sup>43</sup> As the internal stress in the Ag film decreased, we achieved a transition from mono- to bi- to trilayer with transition regions (Figure 3g).

Additionally, to verify the selective separation of the spalled  $\text{MoS}_2$  from their vdW crystal, we performed Raman analysis on the spalled samples. Compared to the reference Raman spectra obtained from mechanically exfoliated  $\text{MoS}_2$ , all spalled  $\text{MoS}_2$  samples exhibited a blue shift in the  $E_{2g}^1$  peak, indicating the

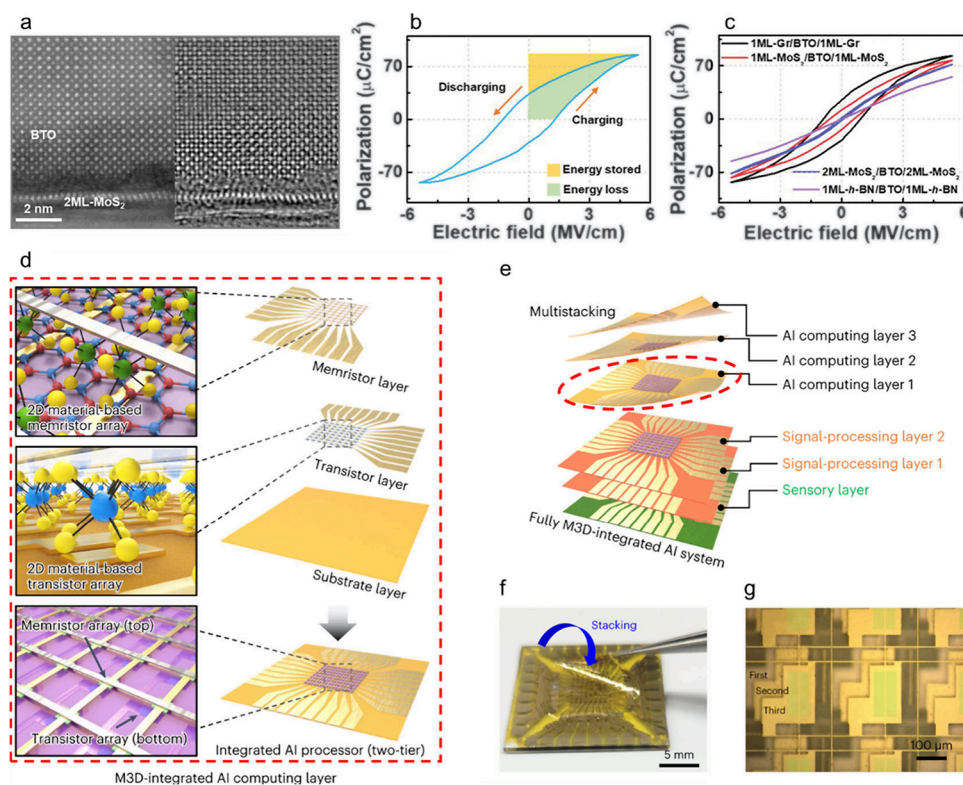


**Figure 5.** Spalled vdW NMs for a high-performance electrostatic capacitor and monolithic integrated AI processor. (a) HAADF-STEM and iDPC-STEM images of bilayer MoS<sub>2</sub>/BTO/bilayer MoS<sub>2</sub> vdW heterostructure. (b, c) P–E curves of pristine BTO and 2D vdW NMs encapsulated in BTO samples. (d, e) Schematic illustrations of an AI processor using monolithically integrated 2D vdW NM-based electronics. The AI processor is composed of a 2D vdW NM-based memristor array and a transistor array. (f, g) Photograph and optical images of three stacks of the AI processor. (Reproduced from refs 46 and 47. Copyrights 2024 AAAS.)

presence of compressive strain originating from Ag stressors (Figure 3h).<sup>44</sup> Remarkably, with increasing crack propagation depth, the E<sub>1<sub>2g</sub></sub> peak of the spalled MoS<sub>2</sub> showed a slight downshift, suggesting a gradual reduction in compressive strain (Figure 3i–k). This observation is consistent with the changes in the internal stress levels of the stressor film.

This precise thickness control of 2D vdW NMs through internal stress modulation of the stressor can also be achieved using nonmetallic stressors.<sup>45</sup> By adjusting the internal stress of a nonmetallic Ge stressor, we successfully peeled off monolayer MoTe<sub>2</sub> from a MoTe<sub>2</sub> vdW crystal and transferred it onto the desired substrate. Furthermore, the water-soluble nature of Ge eliminates the need for a harsh wet chemical etching processes, unlike metal stressors. These results have the potential to be widely employed for the fabrication of high-quality monolayer TMDCs, offering a versatile approach for the chemically unstable 2D vdW NMs. This is particularly beneficial for materials that are difficult to produce in monolayers due to unavoidable surface oxidation and physical damage during metal film removal.

#### 4. APPLICATIONS OF ATOMICALLY PRECISE SPALLED vdW NM

We have delved deeply into advanced spalling strategies designed to overcome recent synthetic challenges associated with vdW NMs in the previous section. After these challenges are addressed through sophisticated spalling techniques, pristine NMs can be utilized to design the proof-of-concept device and explore interesting phenomena across various fields. This section highlights the applications of atomically precise

spalled vdW NMs in different domains. Three notable examples are presented below.

##### 4.1. 2D Crystallographic Scanner

Crystallographic information such as crystallographic orientation and grain boundaries (GBs) plays a pivotal role in determining the properties of 2D vdW NMs. Therefore, for the practical utilization of as-grown 2D vdW NMs, methods to analyze these structural aspects should be developed.

Recently, our group developed a vdW assembling–disassembling technique based on an atomic precision spalling technique, which was utilized for the nondestructive crystallographic scanning of 2D vdW NMs (Figure 4a).<sup>4</sup> This method can unambiguously determine both the GBs and grain structures within 2D vdW NMs. Similar to how a commercial sticky note can be readily attached and detached, two monolayers of graphene can be assembled and disassembled. When monolayer polycrystalline graphene (PCG) and single-crystalline graphene (SCG) are assembled, the hidden GBs and individual grains within the PCG are visualized through twist angle ( $\theta$ )-dependent interlayer electron–phonon interactions with the underlying SCG, resulting in differences in the Raman signal according to each grain.<sup>46</sup> Figure 4b shows the Raman mapping images of assembled PCG/SCG, revealing the distinct distribution of grains and GBs within the PCG. After the grains were effectively identified, the PCG was non-destructively disassembled from the SCG by adjusting the binding energy of the stressor. The excellent uniformity and chemical cleanliness of the disassembled graphene were confirmed by various microscopic and spectroscopic tools, including atomic force microscopy (AFM) and X-ray photo-

electron spectroscopy (XPS) analysis (Figure 4c,d). Moreover, thanks to the contaminant-free and atomically smooth surface of the disassembled SCG, it can be reserved as the template for crystallographic scanning, thus facilitating multiple crystallographic scans on the same SCG sample (Figure 4e–i).

#### 4.2. Enhanced Electrostatic Capacitor

For high-performance electrostatic capacitors without energy loss, materials with a high maximum polarization and low remnant polarization are required. Ferroelectric materials such as  $\text{HfO}_2$ ,  $\text{ZrO}_2$ , and  $\text{BaTiO}_3$  typically provide high maximum polarization, but their high remnant polarization limits the effectiveness of energy storage. To address this, atomically precise spalled 2D vdW NMs can be employed to encapsulate ferroelectric 3D vdW NMs.<sup>47</sup> This creates a 2D/3D/2D vdW heterostructure with sharp interfaces, minimizing energy dissipation and finely controlling relaxation time, thereby effectively suppressing remnant polarization while maintaining maximum polarization.

Unlike conventional heterostructures that suffer from lattice distortion and thermal mismatch issues, this structure preserves the crystallinity of single-crystalline ferroelectric materials, thereby maintaining maximum polarization (Figure 5a). Additionally, the weakly bonded vdW interfaces promote a substantial enhancement in dielectric relaxation, effectively decreasing the extent of remnant polarization (Figure 5b,c).

In particular, the  $\text{MoS}_2/\text{BTO}/\text{MoS}_2$  structure shows low dielectric loss and efficient relaxation time control, outperforming other vdW 2D NMs such as h-BN and graphene (Figure 5c). Notably, bilayer  $\text{MoS}_2$  is more advantageous than monolayer  $\text{MoS}_2$ , as it shows a higher relaxation time and decreased dielectric loss. This improvement is attributed to the lower conductivity at the 2D/3D interface, which offers better charge screening capabilities. Consequently, this structure achieves an impressive energy density of  $191.7 \text{ J/cm}^3$  with over 90% efficiency. This high efficiency addresses the energy dissipation of dielectrics, making it promising for high-power applications.

#### 4.3. Monolithic Integrated AI Processor

In addition, 2D vdW NMs obtained through advanced spalling can be vertically integrated to create monolithic AI processors with a high degree of integrability and multifunctionality (Figure 5d,e).<sup>48</sup> As the core components,  $\text{WSe}_2/\text{hBN}$ -based memristors for storing and computing information and  $\text{MoS}_2$ -based transistors as driving circuitry to control switching behavior were successfully fabricated using the advanced spalling technique. The individual memristor layers showed good endurance under more than 1000 cycles of the set–reset process, and the transistor layers exhibited uniform transfer characteristics with a field-effect mobility of  $10.42 \pm 2.1 \text{ cm}^2/(\text{V s})$  and a subthreshold swing of  $0.612 \pm 0.05 \text{ V/dec}$ . To perform AI tasks, the memristor layer was vertically assembled onto the transistor layer to realize a 1-transistor-1-memristor structure. In total, three layers of transistor and memristor stacks were successfully integrated into a 3D nanosystem (Figure 5f,g). The system was successfully applied for DNA motif discovery using one-dimensional convolution, demonstrating precise control of multiple conductance states through the gate voltage modulation of  $\text{MoS}_2$ -based transistors. This integration improved latency, reduced the voltage drop, and minimized the footprint with high density and reduced surface area.

## 5. CONCLUSIONS AND OUTLOOK

In this Account, we have outlined state-of-the-art atomic precision spalling techniques for producing high-quality vdW NMs, specifically highlighting our recent contribution and significant advancements in this field. Despite the considerable progress in advanced spalling techniques in recent years, several challenges should be addressed for these methods to be extensively adopted for fabricating high-quality vdW NMs as a future technology.

First, automation is needed for the reliable and reproducible production of vdW NMs. Currently, the advanced spalling process heavily relies on tedious and labor-intensive manual handling. Although the theoretical framework and working mechanism of advanced spalling are well established, this manual process could compromise the desired atomic-level control of advanced spalling. Several issues such as unsatisfactory yields (partial exfoliation or mechanical failures) and parasitic cracks resulting in irregular thickness and rough surfaces generally stem from these manual processes. Implementing an automated system with consistent applied bending moments and accurate control over displacement rates during crack propagation could effectively mitigate these issues and provide an optimal condition for the deterministic fabrication of vdW NMs.

Second, further development of stressor materials is essential for the universal production of high-quality vdW NMs. Typically, metal films such as Ni, Au, and Ag are used as stressor materials, and their removal process often requires harsh acid-based etching processes (e.g.,  $\text{FeCl}_3$ ,  $\text{KI}/\text{I}_2$  solution), which can lead to unavoidable contamination on the surface of vdW NMs and damage to their lattice structure, particularly in chemically unstable 2D vdW NMs. Recently, our group developed a water-soluble Ge thin film as a stressor material, which eliminates the need for wet chemicals, showing potential for universal application. However, there is still room for improvement. Preferably, processes that circumvent the need for wet processing should be developed. Self-release-type stressors or stamp-type stressors that can mechanically release after the spalling process, thereby avoiding the need for any stressor etching process, could serve as a viable solution to these challenges.

Additionally, refining our understanding of the interfacial properties, particularly the binding energy between the stressors and the source materials, can further enhance the precision of the spalling process. A deeper exploration of chemical interactions at the interface will lead to the development of more effective stressors and surface treatments. This advancement in chemical understanding is crucial, as it directly impacts the precision of thickness control and the atomic-level smoothness of the spalled layers, ultimately improving the quality and performance of vdW NMs.

Finally, since the intrinsic properties of vdW NMs are directly dependent on the intrinsic properties of their source materials, the co-development of controllable synthesis methods for source materials (e.g., control in composition, doping concentration, and magnitude of intrinsic lattice defects) alongside the progress in the advanced spalling technique is necessary.

## AUTHOR INFORMATION

### Corresponding Authors

**Sang-Hoon Bae** – Mechanical Engineering and Materials Science and Institute of Materials Science and Engineering, Washington University in St. Louis, St. Louis, Missouri 63130, United States; [orcid.org/0000-0002-1518-7635](https://orcid.org/0000-0002-1518-7635); Email: [sbae22@wustl.edu](mailto:sbae22@wustl.edu)

**Jae-Hyun Lee** – Department of Materials Science and Engineering and Department of Energy Systems Research, Ajou University, Suwon 16499, Republic of Korea; [orcid.org/0000-0001-5117-8923](https://orcid.org/0000-0001-5117-8923); Email: [jaehyunlee@ajou.ac.kr](mailto:jaehyunlee@ajou.ac.kr)

### Author

**Ji-Yun Moon** – Mechanical Engineering and Materials Science, Washington University in St. Louis, St. Louis, Missouri 63130, United States

Complete contact information is available at:  
<https://pubs.acs.org/10.1021/acs.accounts.4c00425>

### Author Contributions

CRedit: **Ji-Yun Moon** conceptualization, writing - original draft, writing - review & editing; **Sang-Hoon Bae** funding acquisition, supervision, writing - review & editing; **Jae-Hyun Lee** conceptualization, funding acquisition, supervision, writing - original draft, writing - review & editing.

### Notes

The authors declare no competing financial interest.

### Biographies

**Ji-Yun Moon** earned her Ph.D. in material science and engineering from the Department of Energy Systems at Ajou University. She is currently a postdoctoral researcher in the Department of Mechanical Engineering and Materials Science at Washington University in St. Louis. Her research interests include the growth and advanced spalling of vdW materials and their heterostructures.

**Sang-Hoon Bae** is an assistant professor at Washington University in St. Louis. He received his Ph.D. degree in the Department of Materials Science and Engineering from the University of California, Los Angeles (UCLA) and was then a postdoctoral research associate at the Massachusetts Institute of Technology (MIT). His current research interests include the production of freestanding single-crystalline vdW nanomembranes and the study of physical coupling in their artificial heterostructures.

**Jae-Hyun Lee** is an associate professor at Ajou University. He received his Ph.D. degree from the SKKU Advanced Institute of Nanotechnology at Sungkyunkwan University. Before joining Ajou University, he was a postdoctoral fellow at Sungkyunkwan University and a researcher at the National Graphene Institute at the University of Manchester. His research focuses on the synthesis of electronic-grade van der Waals materials and the study of the interfaces of vdW nanomaterials with other materials.

## ACKNOWLEDGMENTS

This work was supported by a National Research Foundation of Korea (NRF) grant funded by the Korean government (MSIT) (RS-2024-00346906 and RS-2024-00452558). This work was partially supported by the Technology Innovation Program Development Program (RS-2023-00269589, Development of Thermally Conductive Adhesive Material for the

Monolithic Module of Foldable Displays and Low-Energy High-Speed Curing Process) funded by the Ministry of Trade, Industry & Energy (MOTIE, Korea)

## REFERENCES

- (1) Shim, J.; Bae, S.-H.; Kong, W.; Lee, D.; Qiao, K.; Nezhich, D.; Park, Y. J.; Zhao, R.; Sundaram, S.; Li, X.; Yeon, H.; Choi, C.; Kum, H.; Yue, R.; Zhou, G.; Ou, Y.; Lee, K.; Moodera, J.; Zhao, X.; Ahn, J.-H.; Hinkle, C.; Ougazzaden, A.; Kim, J. Controlled crack propagation for atomic precision handling of wafer-scale two-dimensional materials. *Science* **2018**, *362* (6415), 665–670.
- (2) Moon, J.-Y.; Kim, M.; Kim, S.-I.; Xu, S.; Choi, J.-H.; Whang, D.; Watanabe, K.; Taniguchi, T.; Park, D. S.; Seo, J.; Cho, S. H.; Son, S.-K.; Lee, J.-H. Layer-engineered large-area exfoliation of graphene. *Sci. Adv.* **2020**, *6* (44), eabc6601.
- (3) Moon, J.-Y.; Kim, D.-H.; Kim, S.-I.; Hwang, H.-S.; Choi, J.-H.; Hyeong, S.-K.; Ghods, S.; Park, H. G.; Kim, E.-T.; Bae, S.; Lee, S.-K.; Son, S.-K.; Lee, J.-H. Layer-engineered atomic-scale spalling of 2D van der Waals crystals. *Matter* **2022**, *5* (11), 3935–3946.
- (4) Moon, J.-Y.; Kim, S.-I.; Ghods, S.; Park, S.; Kim, S.; Chang, S.; Jang, H. C.; Choi, J.-H.; Kim, J. S.; Bae, S.-H.; Whang, D.; Kim, T.-H.; Lee, J.-H. Nondestructive Single-Atom-Thick Crystallographic Scanner via Sticky-Note-Like van der Waals Assembling–Disassembling. *Adv. Mater.* **2024**, *36*, 2400091.
- (5) Ajayan, P.; Kim, P.; Banerjee, K. Two-dimensional van der Waals materials. *Phys. Today* **2016**, *69* (9), 38–44.
- (6) Bae, S.-H.; Kum, H.; Kong, W.; Kim, Y.; Choi, C.; Lee, B.; Lin, P.; Park, Y.; Kim, J. Integration of bulk materials with two-dimensional materials for physical coupling and applications. *Nat. Mater.* **2019**, *18* (6), 550–560.
- (7) Kim, Y.; Cruz, S. S.; Lee, K.; Alawode, B. O.; Choi, C.; Song, Y.; Johnson, J. M.; Heidelberger, C.; Kong, W.; Choi, S.; Qiao, K.; Almansouri, I.; Fitzgerald, E. A.; Kong, K.; Kolpak, A. M.; Hwang, J.; Kim, J. Remote epitaxy through graphene enables two-dimensional material-based layer transfer. *Nature* **2017**, *544* (7650), 340–343.
- (8) Liu, Y.; Huang, Y.; Duan, X. Van der Waals integration before and beyond two-dimensional materials. *Nature* **2019**, *567* (7748), 323–333.
- (9) Kim, J. H.; Jeong, J. H.; Kim, N.; Joshi, R.; Lee, G.-H. Mechanical properties of two-dimensional materials and their applications. *J. Phys. D Appl. Phys.* **2019**, *52* (8), No. 083001.
- (10) Novoselov, K. S.; Mishchenko, A.; Carvalho, A.; Castro Neto, A. H. 2D materials and van der Waals heterostructures. *Science* **2016**, *353* (6298), No. aac9439.
- (11) Castellanos-Gomez, A.; Duan, X.; Fei, Z.; Gutierrez, H. R.; Huang, Y.; Huang, X.; Quereda, J.; Qian, Q.; Sutter, E.; Sutter, P. Van der Waals heterostructures. *Nat. Rev. Methods Primers* **2022**, *2* (1), 58.
- (12) Liu, Y.; Weiss, N. O.; Duan, X.; Cheng, H.-C.; Huang, Y.; Duan, X. Van der Waals heterostructures and devices. *Nat. Rev. Mater.* **2016**, *1* (9), 1–17.
- (13) Xia, W.; Dai, L.; Yu, P.; Tong, X.; Song, W.; Zhang, G.; Wang, Z. Recent progress in van der Waals heterojunctions. *Nanoscale* **2017**, *9* (13), 4324–4365.
- (14) Li, X.-L.; Han, W.-P.; Wu, J.-B.; Qiao, X. F.; Zhang, J.; Tan, P.-H. Layer-number dependent optical properties of 2D materials and their application for thickness determination. *Adv. Funct. Mater.* **2017**, *27* (19), No. 1604468.
- (15) Duong, D. L.; Yun, S. J.; Lee, Y. H. van der Waals layered materials: opportunities and challenges. *ACS Nano* **2017**, *11* (12), 11803–11830.
- (16) Novoselov, K. S.; Geim, A. K.; Morozov, S. V.; Jiang, D.; Zhang, Y.; Dubonos, S. V.; Grigorieva, I. V.; Firsov, A. A. Electric field effect in atomically thin carbon films. *Science* **2004**, *306* (5696), 666–669.
- (17) Cai, Z.; Liu, B.; Zou, X.; Cheng, H.-M. Chemical vapor deposition growth and applications of two-dimensional material and their heterostructures. *Chem. Rev.* **2018**, *118* (13), 6091–6133.

- (18) Yoon, J.; Jo, S.; Chun, I. S.; Jung, I.; Kim, H.-S.; Meitl, M.; Menard, E.; Li, X.; Coleman, J. J.; Paik, U.; Rogers, J. A. GaAs photovoltaics and optoelectronics using releasable multilayer epitaxial assemblies. *Nature* **2010**, *465* (7296), 329–333.
- (19) Wong, W.; Sands, T.; Cheung, N.; Kneissl, M.; Bour, D.; Mei, P.; Romano, L.; Johnson, N. M. Fabrication of thin-film InGaN light-emitting diode membranes by laser lift-off. *Appl. Phys. Lett.* **1999**, *75* (10), 1360–1362.
- (20) Bedell, S. W.; Fogel, K.; Lauro, P.; Shahrjerdi, D.; Ott, J. A.; Sadana, D. J. Layer transfer by controlled spalling. *J. Phys. D Appl. Phys.* **2013**, *46* (15), No. 152002.
- (21) Kim, H.; Chang, C. S.; Lee, S.; Jiang, J.; Jeong, J.; Park, M.; Meng, Y.; Ji, J.; Kwon, Y.; Sun, X.; Kong, W.; Kun, H. S.; Bae, S.-H.; Lee, K.; Hong, Y. J.; Shi, J.; Kim, J. Remote epitaxy. *Nat. Rev. Methods Primers* **2022**, *2* (1), 40.
- (22) Evans, A.; Drory, M.; Hu, M. S. The cracking and decohesion of thin films. *J. Mater. Res.* **1988**, *3*, 1043–1049.
- (23) Lee, Y.; Tan, H. H.; Jagadish, C.; Karuturi, S. K. Controlled cracking for large-area thin film exfoliation: working principles, status, and prospects. *ACS Appl. Electron. Mater.* **2021**, *3* (1), 145–162.
- (24) Hutchinson, J. W.; Suo, Z. Mixed mode cracking in layered materials. *Adv. Appl. Mech.* **1991**, *29*, 63–191.
- (25) Bedell, S. W.; Lauro, P.; Ott, J. A.; Fogel, K.; Sadana, D. K. Layer transfer of bulk gallium nitride by controlled spalling. *J. Appl. Phys.* **2017**, *122* (2), No. 025103.
- (26) Ma, K. Y.; Zhang, L.; Jin, S.; Wang, Y.; Yoon, S. I.; Hwang, H.; Oh, J.; Jeong, D. S.; Wang, M.; Chatterjee, S.; Kim, G.; Jang, A.-R.; Yang, J.; Ryu, S.; Jeong, H. Y.; Ruoff, R. S.; Chhowalla, M.; Ding, F.; Shin, H. S. Epitaxial single-crystal hexagonal boron nitride multilayers on Ni (111). *Nature* **2022**, *606*, 88–93.
- (27) Li, J.; Yuan, Y.; Lanza, M.; Abate, I.; Tian, B.; Zhang, X. Nonepitaxial wafer-scale single-crystal 2D materials on insulators. *Adv. Mater.* **2024**, *36* (11), No. 2310921.
- (28) Wang, D.; Luo, F.; Lu, M.; Xie, X.; Huang, L.; Huang, W. Chemical vapor transport reactions for synthesizing layered materials and their 2D counterparts. *Small* **2019**, *15* (40), No. 1804404.
- (29) May, A. F.; Yan, J.; McGuire, M. A. A practical guide for crystal growth of van der Waals layered materials. *J. Appl. Phys.* **2020**, *128* (5), No. 051101.
- (30) Fu, D.; Zhao, X.; Zhang, Y.-Y.; Li, L.; Xu, H.; Jang, A.-R.; Yoon, S. I.; Song, P.; Poh, S. M.; Ren, T.; Ding, Z.; Fu, W.; Shin, T. J.; Shin, H. S.; Pantelides, S. T.; Loh, K. P. Molecular beam epitaxy of highly crystalline monolayer molybdenum disulfide on hexagonal boron nitride. *J. Am. Chem. Soc.* **2017**, *139* (27), 9392–9400.
- (31) Ryu, H.; Park, H.; Kim, J.-H.; Ren, F.; Kim, J.; Lee, G.-H.; Pearton, S. J. Two-dimensional material templates for van der Waals epitaxy, remote epitaxy, and intercalation growth. *Appl. Phys. Rev.* **2022**, *9* (3), No. 031305.
- (32) Bae, S.-H.; Lu, K.; Han, Y.; Kim, S.; Qiao, K.; Choi, C.; Nie, Y.; Kim, H.; Kum, H. S.; Chen, P.; Kong, W.; Kang, B.-S.; Kim, C.; Lee, J.; Baek, Y.; Shim, J.; Park, J.; Joo, M.; Muller, D. A.; Lee, K.; Kim, J. Graphene-assisted spontaneous relaxation towards dislocation-free heteroepitaxy. *Nat. Nanotechnol.* **2020**, *15* (4), 272–276.
- (33) Kim, H.; Lu, K.; Liu, Y.; Kum, H. S.; Kim, K. S.; Qiao, K.; Bae, S.-H.; Lee, S.; Ji, Y. J.; Kim, K. H.; Paik, H.; Xie, S.; Shin, H.; Choi, C.; Lee, J. H.; Dong, C.; Robinson, J. A.; Lee, J.-H.; Ahn, J.-H.; Yeon, G. Y.; Schlom, D. G.; Kim, J. Impact of 2D–3D heterointerface on remote epitaxial interaction through graphene. *ACS Nano* **2021**, *15* (6), 10587–10596.
- (34) Suo, Z.; Hutchinson, J. W. Structures, Steady-state cracking in brittle substrates beneath adherent films. *Int. J. Solids Struct.* **1989**, *25* (11), 1337–1353.
- (35) Schabel, M. C.; Martins, J. L. Energetics of interplanar binding in graphite. *Phys. Rev. B* **1992**, *46* (11), 7185.
- (36) Giovannetti, G.; Khomyakov, P. A.; Brocks, G.; Karpan, V. M.; van den Brink, J.; Kelly, P. J. Doping graphene with metal contacts. *Phys. Rev. Lett.* **2008**, *101* (2), No. 026803.
- (37) Bae, S.-H.; Zhou, X.; Kim, S.; Kim, J. Unveiling the carrier transport mechanism in epitaxial graphene for forming wafer-scale single-domain graphene. *Proc. Natl. Acad. Sci. U. S. A.* **2017**, *114* (16), 4082–4086.
- (38) Yoon, H.; Truttmann, T. K.; Liu, F.; Matthews, B. E.; Choo, S.; Su, Q.; Saraswat, V.; Manzo, S.; Arnold, M. S.; Bowden, M. E.; Kawasaki, J. K.; Koester, S. J.; Spurgeon, S. R.; Chambers, S. A.; Jalan, B. Freestanding epitaxial SrTiO<sub>3</sub> nanomembranes via remote epitaxy using hybrid molecular beam epitaxy. *Sci. Adv.* **2022**, *8* (51), No. eadd5328.
- (39) Kum, H. S.; Lee, H.; Kim, S.; Lindemann, S.; Kong, W.; Qiao, K.; Chen, P.; Irwin, J.; Lee, J. H.; Xie, S.; Subramaniam, S.; Shim, J.; Bae, S.-H.; Choi, C.; Ranno, L.; Seo, S.; Lee, S.; Bauer, J.; Li, H.; Lee, K.; Robinson, J. A.; Ross, C. A.; Schlom, D. G.; Rzczowski, M. S.; Eom, C.-B.; Kim, J. Heterogeneous integration of single-crystalline complex-oxide membranes. *Nature* **2020**, *578* (7793), 75–81.
- (40) Kim, H.; Lee, S.; Shin, J.; Zhu, M.; Akl, M.; Lu, K.; Han, N. M.; Baek, Y.; Chang, C. S.; Suh, J. M.; Kim, K. S.; Park, B.-I.; Zhang, Y.; Choi, C.; Shin, H.; Yu, H.; Meng, Y.; Kim, S.-I.; Seo, S.; Lee, K.; Kum, H. S.; Lee, J.-H.; Ahn, J.-H.; Bae, S.-H.; Hwang, J.; Shi, Y.; Kim, J. Graphene nanopattern as a universal epitaxy platform for single-crystal membrane production and defect reduction. *Nat. Nanotechnol.* **2022**, *17* (10), 1054–1059.
- (41) Moon, J.-Y.; Kim, S.-I.; Josline, M. J.; Kim, C. Y.; Kim, J. S.; Kim, I.; Jung, E.; Lee, J.-H. Protocol for preparing layer-engineered van der Waals materials through atomic spalling. *STAR Protoc.* **2023**, *4* (2), No. 102228.
- (42) Saedi, A.; Rost, M. Thermodynamics of deposition flux-dependent intrinsic film stress. *Nat. Commun.* **2016**, *7* (1), No. 10733.
- (43) Park, H.; Lim, C.; Lee, C.-J.; Choi, M.; Jung, S.; Park, H. Analytical model of spalling technique for thickness-controlled separation of single-crystalline semiconductor layers. *Solid-State Electron.* **2020**, *163*, No. 107660.
- (44) Pak, S.; Lee, J.; Lee, Y.-W.; Jang, A.-R.; Ahn, S.; Ma, K. Y.; Cho, Y.; Hong, J.; Lee, S.; Jeong, H. Y.; Im, H.; Shin, H. S.; Morris, S. M.; Cha, S.; Sohn, J. I.; Kim, J. M. Strain-mediated interlayer coupling effects on the excitonic behaviors in an epitaxially grown MoS<sub>2</sub>/WS<sub>2</sub> van der Waals heterobilayer. *Nano Lett.* **2017**, *17* (9), 5634–5640.
- (45) Kim, S.; Kim, S.-I.; Ghods, S.; Kim, J.-S.; Lee, Y. C.; Kwun, H. J.; Moon, J.-Y.; Lee, J.-H. Nonmetal-Mediated Atomic Spalling of Large-Area Monolayer Transition Metal Dichalcogenide. *Small Sci.* **2023**, *3* (9), No. 2300033.
- (46) Eliel, G.; Moutinho, M.; Gadelha, A.; Righi, A.; Campos, L.; Ribeiro, H.; Chiu, P.-W.; Watanabe, K.; Taniguchi, T.; Puech, P.; Paillet, M.; Michel, T.; Venezuela, P.; Pimenta, M. A. Intralayer and interlayer electron–phonon interactions in twisted graphene heterostructures. *Nat. Commun.* **2018**, *9* (1), 1221.
- (47) Han, S.; Kim, J. S.; Park, E.; Meng, Y.; Xu, Z.; Foucher, A. C.; Jung, G. Y.; Roh, I.; Lee, S.; Kim, S. O.; Moon, J.-Y.; Kim, S.-I.; Bae, S.; Zhang, X.; Park, B.-I.; Seo, S.; Li, Y.; Shin, H.; Reidy, K.; Hoang, A. T.; Sundaram, S.; Vuong, P.; Kim, C.; Zhao, J.; Hwang, J.; Wang, C.; Choi, H.; Kim, D.-H.; Kwon, J.; Park, J.-H.; Ougazzaden, A.; Lee, J.-H.; Ahn, J.-H.; Kim, J.; Mishra, R.; Kim, H.-S.; Ross, F. M.; Bae, S.-H. High energy density in artificial heterostructures through relaxation time modulation. *Science* **2024**, *384* (6693), 312–317.
- (48) Kang, J.-H.; Shin, H.; Kim, K. S.; Song, M.-K.; Lee, D.; Meng, Y.; Choi, C.; Suh, J. M.; Kim, B. J.; Kim, H.; Howang, A. T.; Park, B.-I.; Cho, G.; Sundaram, S.; Vuong, P.; Shin, J.; Choe, J.; Xu, Z.; Younas, R.; Kim, J. S.; Han, S.; Lee, S.; Kim, S. O.; Kang, B.; Seo, S.; Ahn, H.; Seo, S.; Reidy, K.; Park, E.; Mun, S.; Park, M.-C.; Lee, S.; Kim, H.-J.; Kum, H. S.; Lin, P.; Hinkle, C.; Ougazzaden, A.; Ahn, J.-H.; Kim, J.; Bae, S.-H. Monolithic 3D integration of 2D materials-based electronics towards ultimate edge computing solutions. *Nat. Mater.* **2023**, *22* (12), 1470–1477.